Biochemical and Biophysical Research Communications 404 (2011) 546–551

Contents lists available at ScienceDirect

Biochemical and Biophysical Research Communications

journal homepage: www.elsevier.com/locate/ybbrc

Identification of a novel protein, PriB, in *Klebsiella pneumoniae*

Hui-Chuan Hsieh [a], Cheng-Yang Huang [a,b,*]

[a] Department of Biomedical Sciences, Chung Shan Medical University, No. 110, Sec. 1, Chien-Kuo N. Rd., Taichung City, Taiwan
[b] Department of Medical Research, Chung Shan Medical University Hospital, No. 110, Sec. 1, Chien-Kuo N. Rd., Taichung City, Taiwan

ARTICLE INFO

Article history:
Received 2 December 2010
Available online 6 December 2010

Keywords:
PriB
PriA
Primosome
ssDNA binding
SSB

ABSTRACT

PriB is a primosomal protein required for the reinitiation of replication in bacteria. Here, we report the identification and characterization of a novel PriB protein in *Klebsiella pneumoniae* (KPN_04595; *Kp*PriB). Unlike the well-studied *Escherichia coli* PriB protein (*Ec*PriB), which exists as a homodimer comprising 104-aa polypeptides, *Kp*PriB forms a monomer of only 55 aa, due to the absence of the 49 aa N-terminus in *Kp*PriB. Although this N-terminal region (1–49 aa) in *Ec*PriB contains several important residues, such as K18, R34, and W47, which are crucial for ssDNA binding, we found that *Kp*PriB binds ssDNA, but not ssRNA, with comparable affinity as that for *Ec*PriB. Results from filter-binding assays demonstrate that the *Kp*PriB–ssDNA interaction is cooperative and salt-sensitive. Substituting the residue K33 in *Kp*PriB with alanine, the position corresponding to the classic ssDNA-binding residue K82 of *Ec*PriB located in loop L_{45}, significantly reduced ssDNA-binding activity and cooperativity. These results reveal that the 1–49 aa region of the classical PriB protein is unnecessary for ssDNA binding. On the basis of these findings, the structure–function relationships of *Kp*PriB are discussed.

1. Introduction

The ability to reinitiate replication after DNA damage is essential for bacterial survival [1,2]. The replication restart primosome is a multi-protein complex that reactivates stalled DNA replication at the forks after DNA damage [3–5]. In *Escherichia coli*, the primosome includes 7 essential proteins (PriA, PriB, PriC, DnaB, DnaC, DnaT, and DnaG). There are 2 overlapping mechanisms for reassembly of the replication forks; initiation is induced by either PriA helicase or PriC [6–8]. In the PriA-directed pathway, PriB is the second protein to be assembled in the protein–DNA complex [9], where it then stimulates PriA helicase activity [10]. PriB also stabilizes the binding of PriA to DNA hairpins and therefore facilitates the association of DnaT with the primosome [11]. In an ATP- and DnaC-dependent manner, DnaB helicase is then loaded onto the complex and forms the complete primosome upon binding with DnaG primase [12–14]. Recruitment of DnaB helicase to the DNA results in reactivation of the repaired replication forks, allowing bidirectional DNA synthesis to resume.

PriB exists as a homodimer [15–18] with 104-aa polypeptide chains. The PriB monomer has an oligonucleotide/oligosaccharide binding (OB)-fold structure [19,20], and it can bind both ssDNA and ssRNA [18]. The DNA-binding site of PriB is located in loop L_{45} centrally within the dimer [21], and this site occupies 12 ± 1 nt of the total site-size [22]. Furthermore, PriB shares structural similarity with the DNA-binding domain of *E. coli* ssDNA-binding protein (*Ec*SSB) [16–18,23,24], but they differ in their ssDNA-binding modes [21,22].

While significant progress has been made in understanding the structure and function of *Ec*PriB, study of these proteins in other bacterial species is limited. Many prokaryotic genomes do not contain the full component of the primosome genes [15]. In addition, several PriBs, such as *Kp*PriB, *Pc*PriB, and *Yr*PriB from *Klebsiella pneumoniae*, *Pectobacterium carotovorum* (*Pc*), *Yersinia ruckeri* (*Yr*), and *Salmonella enterica* (*Se*) are shorter in length than *Ec*PriB, specifically lacking the N-terminal 1–49 aa fragment present in *Ec*PriB (Fig. 1A). This N-terminal region in *Ec*PriB contains several important residues for binding to other primosomal proteins and ssDNA, and for dimerization [9,15]. Therefore, the PriBs lacking such a region must have mechanisms for primosome assembly that are distinct from that of *Ec*PriB.

Previously, we described the crystal structures of *Ec*PriB [18] and its complex with ssDNA [21]. Here, we aimed to determine whether the shorter 55-aa PriB polypeptides bind ssDNA and dimerize. In order to do so, *KPN_04595*, the gene encoding a putative PriB from *K. pneumoniae* was cloned and expressed, and its

Abbreviations: ssDNA, single-stranded DNA; SSB, single-stranded DNA-binding protein; EMSA, electrophoretic mobility shift analysis; nt, nucleotides; aa, amino acids; K_d, the apparent dissociation constant; OB, oligonucleotide/oligosaccharide binding; *Ec*SSB, *E. coli* ssDNA-binding protein.

* Corresponding author at: Department of Biomedical Sciences, Chung Shan Medical University, No. 110, Sec. 1, Chien-Kuo N. Rd., Taichung City, Taiwan. Fax: +886 4 23248187.
E-mail address: cyhuang@csmu.edu.tw (C.-Y. Huang).

0006-291X/$ - see front matter © 2010 Elsevier Inc. All rights reserved.
doi:10.1016/j.bbrc.2010.12.023

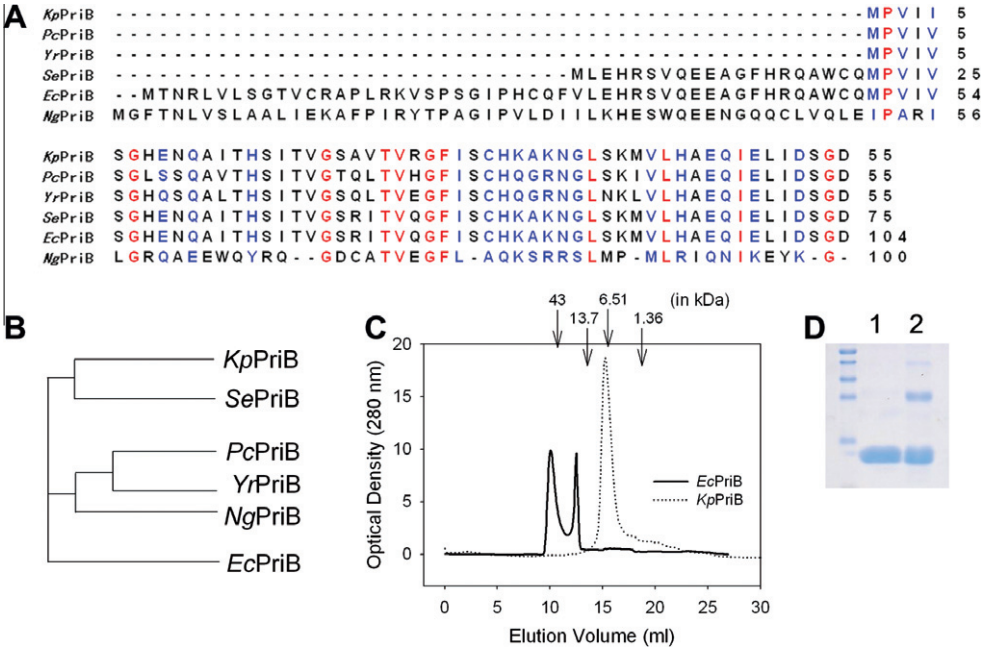

Fig. 1. (A) Multiple amino acid sequence alignment of PriB from *K. pneumoniae* (*Kp*), *P. carotovorum* (*Pc*), *Y. ruckeri* (*Yr*), *S. enterica* (*Se*), *E. coli* (*Ec*), and *Neisseria gonorrhoeae* (*Ng*). Alignment was carried out using CLUSTALW2. Amino acid residues displaying 100% homology are highlighted in red, and those displaying similarity are highlighted in blue. (B) The evolutionary tree of these PriB proteins was generated by CLUSTALW2. (C) Gel-filtration chromatographic analysis of *Kp*PriB and *Ec*PriB is shown. Two peaks are found for *Ec*PriB at 10 mg/ml, whereas only a single peak is found for *Kp*PriB under the same conditions. (D) Analysis of the subunit structure of *Kp*PriB (20 μM) assessed by glutaraldehyde (1%) chemical cross-linking in the absence (lane 1) and presence of 5 μM dT30 (lane 2). Retarded species have mobilities consistent with the formation of cross-linked dimers (~15 kDa) and tetramers of *Kp*PriB (~30 kDa). The sizes of the standard proteins, from the top down, are as follows: 40, 35, 25, 15, and 10 kDa. (For interpretation of the references to colour in this figure legend, the reader is referred to the web version of this article.)

gene product was purified and biophysically characterized. Site-directed mutagenesis of the putative DNA-binding residue of *Kp*PriB was also performed, and the structure–function relationship of this novel PriB was elucidated.

2. Materials and methods

2.1. Materials

All restriction enzymes and DNA-modifying enzymes were purchased from New England Biolabs (Ipswich, MA, USA) unless explicitly stated otherwise. All chemicals were purchased from Sigma–Aldrich (St. Louis, MO, USA) unless explicitly stated otherwise. The *E. coli* strains TOP10F′ (Invitrogen, USA) and BL21(DE3)pLysS (Novagen, UK) were used for genetic construction and protein expression, respectively.

2.2. Construction of the KpPriB expression plasmid

KPN_04595, the gene encoding the putative *Kp*PriB, was PCR-amplified using genomic DNA of *K. pneumoniae* subsp. *pneumoniae* MGH 78578 as the template. The forward (5′-GCCGCGAATTCCC CGTTATTATTAGCG-3′) and reverse (5′-GCGGCAAGCTTGTCTCCAGA ATCTATC-3′) primers were designed to introduce unique *Eco*RI and *Hind*III restriction sites (underlined) into *Kp*PriB, permitting the insertion of the amplified gene into the pET21e vector. The pET21e vector was engineered from the pET21b vector (Novagen Inc., Madison, WI, USA), to avoid having the N-terminal T7 tag fused with the gene product [25]. Therefore, the expected gene product expressed by pET21e–*Kp*PriB will have 2 additional artificial residues, EF, introduced by the *Eco*RI site located at the N-terminus, and a C-terminal His tag (KLAAALEHHHHHH), useful for purifying the recombinant protein.

2.3. Site-directed mutagenesis

The *Kp*PriB K33A mutant was generated according to the QuikChange Site-Directed Mutagenesis kit protocol (Stratagene; LaJolla, CA, USA), by using the forward (5′-GGTTCATCTCTTGCCATGC GGCAAAGAACGGCTTGAGC-3′) and the reverse (5′-TGCTCAAGCCGT TCTTTGCCGCATGGCAAGAGATGAACC-3′) primers, and the wild-type plasmid pET21e–*Kp*PriB as a template. The presence of the mutation was verified by DNA sequencing.

2.4. Protein expression and purification

Recombinant wild-type and mutant *Kp*PriB proteins were expressed and purified using the same protocol as described previously for *Ec*PriB [18]. Briefly, *E. coli* cells were transformed with the wild-type or mutant pET21e–*Kp*PriB plasmids and grown to 0.9 OD_{600} at 37 °C in Luria–Bertani medium containing 250 μg/ml ampicillin with rapid shaking. Overexpression of the *Kp*PriB constructs was induced by incubating with 1 mM isopropyl thiogalactoside (IPTG) for 3 h at 37 °C. The cells overexpressing the protein were chilled on ice, harvested by centrifugation, resuspended in Buffer A (20 mM Tris–HCl, 5 mM imidazole, 0.5 M NaCl; pH 7.9) and disrupted by sonication with ice cooling between pulses. The wild-type and mutant *Kp*PriB proteins were purified from the soluble supernatant by Ni^{2+}-affinity chromatography (HiTrap HP; GE Healthcare Bio-Sciences, Piscataway, NJ, USA).

2.5. Gel filtration

Gel-filtration chromatography was carried out by using an AKTA-FPLC system [26]. Briefly, purified *Kp*PriB (10 mg/ml) and *Ec*PriB (10 mg/ml) in buffer (0.1 M NaCl and 20 mM Tris–HCl at pH 7.9) was applied to a Superdex 75 10/300 GL column (GE

Healthcare Bio-Sciences, Piscataway, NJ, USA) equilibrated with the same buffer. The column was operated at a flow rate of 0.5 mL/min, and 0.5-mL fractions were collected. The protein was detected by measuring absorbance at 280 nm. The column was calibrated with samples of known molecular masses: BSA (67 kDa), ovalbumin (43 kDa), ribonuclease A (13.7 kDa), aprotinin (6.512 kDa), and vitamin B_{12} (1.355 kDa) (GE Healthcare Bio-Sciences, Piscataway, NJ, USA).

2.6. Gel shifts

Various lengths of ssDNA oligonucleotides were custom synthesized by MdBio, Inc., Frederick, MD. RNA oligonucleotides (U30 and A30) were obtained from Dharmacon, Inc., Lafayette, CO (Thermo Fisher Scientific). Radiolabeling was carried out with [γ^{32}P]ATP (6000 Ci/mmol; PerkinElmer Life Sciences) and T4 polynucleotide kinase (Promega, Madison, WI, USA). *Kp*PriB (0, 0.2, 0.4, 0.8, 1.6, 3.2, 6.4, 12.5, 25, and 50 μM) were incubated for 30 min at 25 °C with 1.7 nM DNA or RNA substrates (dT5–60, dA30, dC30, rA30, and rU30) in a total volume of 10 μL in 20 mM Tris–HCl pH 8.0 and 100 mM NaCl. Aliquots (5 μL) were removed from each reaction solution and added to 2 μL of gel-loading solution (0.25% bromophenol blue and 40% sucrose). The resulting samples were resolved on a native 8% polyacrylamide gel at 4 °C in TBE buffer (89 mM Tris borate and 1 mM EDTA) for 1 h at 100 V and visualized by autoradiography. Complexed and free DNA or RNA bands were scanned and quantified.

2.7. Filter binding assay

The affinity of *Kp*PriB for ssDNA was examined by a double-filter binding assay using the same protocol as described previously for *Ec*PriB [21,27]. Briefly, ssDNA–*Kp*PriB complexes were generated by incubating 1 nM of ^{32}P-labeled oligonucleotide with various concentrations of *Kp*PriB (10^{-5}–10^{-9} M) for 30 min at 25 °C in binding buffer containing 50 mM Hepes, pH 7.0, and 40 μg/ml BSA. The reaction mixture, in a total volume of 50 μL, was filtered though a nitrocellulose membrane overlaid on a Hybond N+ nylon membrane (GE Healthcare Bio-Sciences, Piscataway, NJ, USA). The membranes have been pre-soaked for 10 min in a washing buffer containing 50 mM Hepes, pH 7.0, and 10 mM NaCl, before being framed into a dot-blotting apparatus. The slots were washed immediately with 100 μL of washing buffer before and after the sample filtering step. The radioactivity on both filters was quantified with a PhosphorImager (Molecular Dynamics), and the fraction of bound ssDNA was estimated.

2.8. Data analysis

Apparent dissociation constants were determined by plotting the fraction of ssDNA bound at each protein concentration and then fitting the data to the following equation: $\theta = [P]/([P] + K_d)$, in which θ is the fraction of ssDNA bound, [P] is the concentration of total protein, and K_d is the apparent dissociation constant. Cooperative binding to ssDNA sites was assessed by plotting the fraction of ssDNA bound over a range of protein concentrations, and the binding data were analyzed by fitting the data to the following equation: $\log(\theta/(1-\theta)) = h \log[P] - h \log K_d$, where h is the Hill coefficient [21,28].

2.9. Glutaraldehyde cross-linking

*Kp*PriB (20 μM) was incubated in the presence or absence of 5 μM dT30 for 10 min, and then added 1% glutaraldehyde for a further 2 min. The reaction was quenched by the addition of 1 M Tris (pH 8.0), and the cross-linked protein solutions were then analyzed after SDS–PAGE (15%).

3. Results and discussion

3.1. Sequence analysis

The gene *KPN_04595* encoding the putative *Kp*PriB is described in the NCBI database. Based on the known nucleotide sequence, the predicted *Kp*PriB monomer protein has a length of 55 aa and a molecular mass of 7 kDa. This differs from the well-studied 104-aa *Ec*PriB protein. Analysis of the primary structure of *Kp*PriB by RPS-BLAST [29] revealed the presence of an RPA OB fold-like domain. Fig. 1A shows alignment of the amino acid sequences of *K. pneumoniae*, *P. carotovorum* (*Pc*), *Y. ruckeri* (*Yr*), *S. enterica* (*Se*), *E. coli*, and *Neisseria gonorrhoeae* (*Ng*) PriB. The primary structures of these PriBs are similar; however, *Kp*PriB, *Pc*PriB, *Yr*PriB, and *Se*-PriB are shorter in length than *Ec*PriB and *Ng*PriB. Specifically, the N-terminal 1–49 aa region of *Ec*PriB is absent in *Kp*PriB. This region in *Ec*PriB contains several important residues crucial for ssDNA binding, such as K18, R34, and W47 [17,21]. In addition, the W47 residue of *Ec*PriB has been proven to stimulate PriA helicase [10]. These residues, conserved in most PriB families [15], are not found in *Kp*PriB, *Pc*PriB, and *Yr*PriB, due to their truncated gene products. The evolutionary tree for these PriBs is shown: they could be classified into at least 3 groups (Fig. 1B).

3.2. Oligomerization of KpPriB in solution

To determine whether the length of the gene product affects its oligomerization state, we analyzed *Kp*PriB and *Ec*PriB by gel filtration chromatography. As shown in Fig. 1C, *Ec*PriB exists as a dimer and a tetramer (solid line) [16]. However, analysis of purified *Kp*PriB by gel filtration chromatography revealed a single peak (dotted line). Assuming that *Kp*PriB has a structure and partial specific volume similar to the standard proteins, the native molecular mass of *Kp*PriB was estimated to be ~7 kDa. Thus, the single peak suggests that *Kp*PriB, unlike *Ec*PriB, is a stable monomer.

To assess whether *Kp*PriB forms dimer or oligomer in the presence of ssDNA, we incubated the protein with glutaraldehyde in order to cross-link lysine residues in the presence and absence of dT30. As shown in Fig. 1D, addition of dT30 resulted in a significant increase in the amount of cross-linked species, which may correspond to the presence of dimers (~15 kDa) and tetramers (~30 kDa) of *Kp*PriB. Taken together with the gel filtration data (Fig. 1C), these studies suggest that *Kp*PriB is a monomer in solution, and that oligomers (mainly dimers) are formed, only in the presence of ssDNA.

3.3. KpPriB binds ssDNA

To assess whether *Kp*PriB binds ssDNA, we assessed binding of *Kp*PriB to dT20 (Fig. 2A), dT25 (Fig. 2B), dT30 (Fig. 2C), dT35 (Fig. 2D), dT40 (Fig. 2E), dT45 (Fig. 2F), dT50 (Fig. 2G), dT55 (Fig. 2H), and dT60 (Fig. 2I) with different protein concentrations using EMSA. As shown in Fig. 2A, no significant band shift was observed when *Kp*PriB was incubated with dT20, indicating that *Kp*PriB could not form a stable complex with dT20 during electrophoresis. In contrast to dT20, the longer dT homopolymers bind to *Kp*PriB, forming a single complex (Fig. 2B–I). These interactions appear to be highly cooperative since only 1 complex of *Kp*PriB molecules bound per ssDNA is visible when the length of the dT homopolymers is further increased to 60 nt; there is no other distinctive complex or intermediate form. Thus, the shorter *Kp*PriB can bind ssDNA, and the length of ssDNA required for forming a

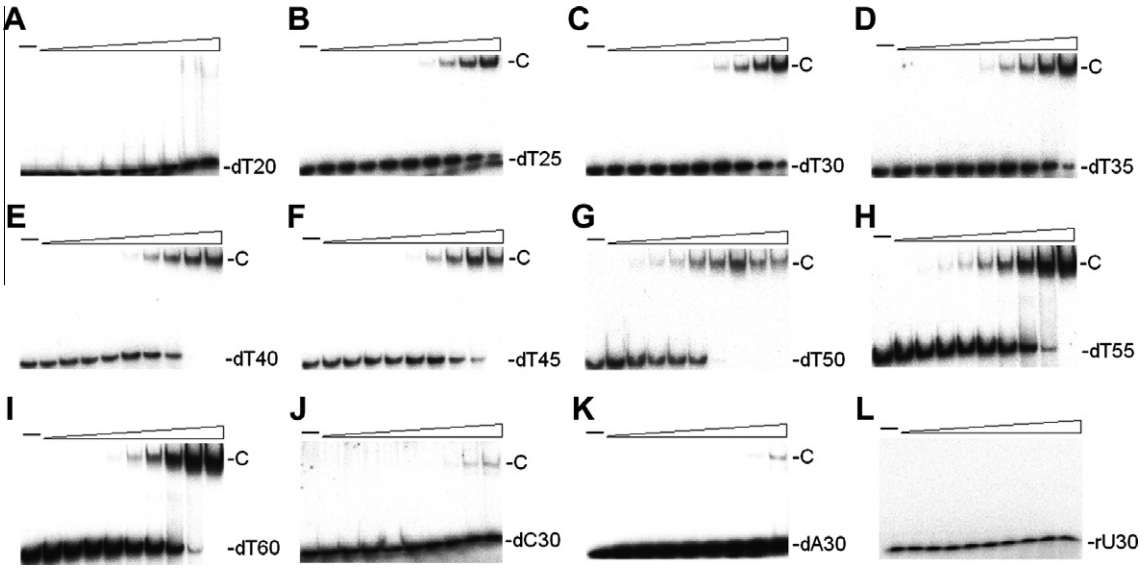

Fig. 2. *Kp*PriB binding affinities to (A–I) dT20–60, (J) dC30, (K) dA30, and (L) U30. The reaction solutions contain 1.7 nM of the oligonucleotide and *Kp*PriB (0–50 μM).

stable complex with *Kp*PriB molecule(s) is approximately 25 nt, as determined using EMSA.

3.4. Base preference for ssDNA binding of KpPriB

To test the base preference for *Kp*PriB binding to purine and pyrimidine, we used dT30 (Fig. 2C), dC30 (Fig. 2J), and dA30 (Fig. 2K) to bind to *Kp*PriB. Like *Ec*PriB [18], *Kp*PriB shows a higher preference for dT30 than for dA30. In addition, this study revealed that the binding preference of *Kp*PriB follows the given order: dT > dC > dA, i.e., *Kp*PriB preferentially binds to pyrimidine than to purine. However, the *in vitro* base preference of PriB, as well as other SSBs [30], is still unknown.

3.5. RNA binding activity of KpPriB

It has been previously reported that *Ec*PriB binds ssRNA (U35) with an affinity that is comparable to its affinity for ssDNA dT35 [18]. In order to assess whether the ability of PriB to bind to RNA is conserved, we assessed the binding of rU30 (Fig. 2L) and dT30 (Fig. 2C) to *Kp*PriB. Unexpectedly, *Kp*PriB did not bind to rU30 with the same affinity as it did for dT30. Thus, the RNA-binding activity of PriB among different species is not conserved and therefore is likely to be unnecessary in the *K. pneumoniae* primosome assembly.

3.6. Cooperative binding of KpPriB to ssDNA

The ssDNA binding ability of *Kp*PriB was studied via a filter-binding assay using dT15. Since dT20 or longer homopolymers give high background noise on binding to nitrocellulose filters, they were excluded from the assays. The titration curves for *Kp*PriB are shown in Fig. 3, and the estimated apparent K_d values are summarized in Table 1. The binding affinity of *Kp*PriB for dT15 (filled circle) increased significantly within a narrow range of protein concentrations, indicating that the formation of the *Kp*PriB–dT15 complex is a positive cooperative process. The Hill coefficient (h) for *Kp*PriB–dT15 binding was determined to be 3.41 ± 0.56, which is significantly higher than that for *Ec*PriB–dT15 (1.5 ± 0.1) [21]. The strong cooperative binding of *Kp*PriB to ssDNA has important implications for the nature of the protein–protein interactions within the complex and the position of the ssDNA-binding sites on *Kp*PriB. This is especially important considering that *Kp*PriB lacks several important residues for ssDNA binding, as compared with *Ec*PriB [9,17,18,21].

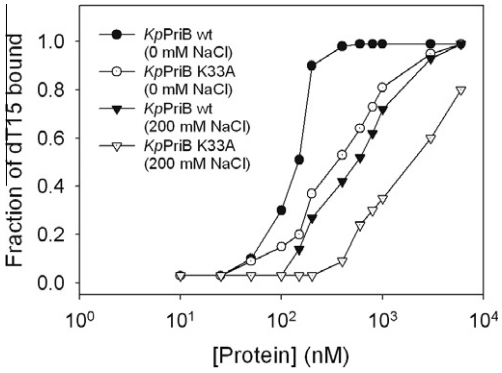

Fig. 3. Filter-binding assay. Titration curves of increasing amounts of *Kp*PriB and the mutant K33A assayed in the absence or presence of 200 mM NaCl, respectively.

Table 1
ssDNA-binding parameters of *Kp*PriB.

	[NaCl] (mM)	Apparent K_d (nM)	h
*Kp*PriB wt	0	140 ± 20	3.41 ± 0.56
*Kp*PriB K33A	0	380 ± 20	1.26 ± 0.08
*Kp*PriB wt	200	580 ± 50	1.33 ± 0.12
*Kp*PriB K33A	200	2600 ± 400	1.28 ± 0.19

The errors are standard deviations determined using 2–4 independent titration experiments.

3.7. Salt effect on ssDNA binding of KpPriB

The ssDNA-binding surface of *Ec*PriB is highly electropositive and interacts directly with both the bases and the phosphate back-

bone of ssDNA [21]. Although *Kp*PriB lacks the N-terminal 1–49 aa region seen in *Ec*PriB, the most important residues for ssDNA binding, K33, K35, and K40, corresponding to positions K82, K84, and K89, respectively, in *Ec*PriB, are conserved [21]. To investigate whether the electrostatic interactions play a role in ssDNA binding, we examined the binding of *Kp*PriB to dT15 at high salt concentrations (200 mM NaCl). As expected, the binding affinity of *Kp*PriB for dT15 is salt dependent, and is approximately 4-fold lower than that measured in the absence of salt (Table 1). Furthermore, the Hill coefficient (h) is reduced to 1.26 ± 0.08, indicating lower cooperativity in these conditions.

3.8. Role of K33 in KpPriB–ssDNA binding

To investigate the contribution of K33 in *Kp*PriB–ssDNA binding, a mutant was created with an alanine substitution at the position corresponding to K82 in loop L_{45} of *Ec*PriB. Binding was assessed in the absence (open circle) and presence of 200 mM NaCl (open triangle) (Fig. 3). As shown in Table 1, the K33A mutant has a K_d value (380 ± 20 nM) that is 2.7-fold higher than that of the wild-type *Kp*PriB (140 ± 20 nM) in the absence of additional NaCl. In the presence of 200 mM NaCl, the K33A mutant has a K_d value (2600 ± 400 nM) that is ~19-fold higher than that of the wild-type *Kp*PriB assayed without additional salt. The Hill coefficient of the K33A mutant is 1.26 ± 0.08 and 1.28 ± 0.19, when in the absence and presence of 200 mM NaCl, respectively. These data indicate that *Kp*PriB binds to ssDNA mainly through electrostatic interactions, especially within the positive charge region. Hence, the K33 position in *Kp*PriB appears to be involved not only in ssDNA binding, but also in the intra- or/and inter-molecular cooperative binding to other residue(s) of *Kp*PriB.

3.9. Comparison with EcPriB

The homodimeric arrangement of OB folds in *Ec*PriB (Fig. 4A) is roughly conserved among known PriB homologs. In this study, we reported a novel PriB from *K. pneumoniae* that is shorter and monomeric compared with the known PriBs, which are polymeric. It has been previously reported that the monomeric interactions found in the *Ec*PriB dimer are tightly packed by hydrophobic interactions [16–18] involving the residues Leu5, Leu7, Met50, and Ile78. Two of these residues, Met1 and Ile29, exist in the shorter *Kp*PriB homolog (Fig. 1A). The lack of the 2 Leu residues results in the failure to homodimerize (Figs. 1C and 4B), but the remaining residues are sufficient for mediating ssDNA binding (Figs. 2–4).

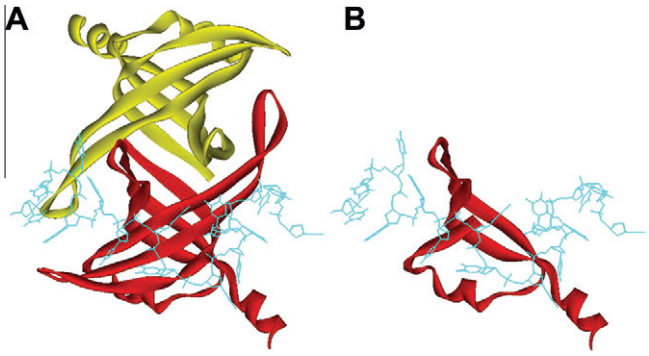

Fig. 4. (A) Crystal structure of *Ec*PriB complexed with ssDNA (derived from PDB code 2CCZ) [21]. A ribbon diagram reveals individual monomers (in gold and red) and ssDNA (cyan). (B) The residues of *Ec*PriB present in *Kp*PriB are shown. (For interpretation of the references to colour in this figure legend, the reader is referred to the web version of this article.)

Previous investigations of *Ec*PriB demonstrated that aromatic stacking, mediated by residues Phe42 and Trp47, plays an important role in ssDNA binding and in stimulating PriA helicase [10]. These residues, however, do not exist in *Kp*PriB. Therefore, the mechanisms and the binding modes of *Kp*PriB, as well as other *K. pneumoniae* primosomal proteins, to ssDNA remain to be explored.

Acknowledgment

This research was supported a grant from the National Research Program for Genome Medicine (NSC 99-3112-B-040-001 to C.Y. Huang).

References

[1] R.C. Heller, K.J. Marians, Replisome assembly and the direct restart of stalled replication forks, Nat. Rev. Mol. Cell Biol. 7 (2006) 932–943.
[2] M.M. Cox, M.F. Goodman, K.N. Kreuzer, D.J. Sherratt, S.J. Sandler, K.J. Marians, The importance of repairing stalled replication forks, Nature 404 (2000) 37–41.
[3] P. McGlynn, R.G. Lloyd, Recombinational repair and restart of damaged replication forks, Nat. Rev. Mol. Cell Biol. 3 (2002) 859–870.
[4] S.J. Sandler, K.J. Marians, Role of PriA in replication fork reactivation in *Escherichia coli*, J. Bacteriol. 182 (2000) 9–13.
[5] K.J. Marians, PriA-directed replication fork restart in *Escherichia coli*, Trends Biochem. Sci. 25 (2000) 185–189.
[6] H. Masai, T. Tanaka, D. Kohda, Stalled replication forks: making ends meet for recognition and stabilization, Bioessays 32 (2010) 687–697.
[7] C.B. Gabbai, K.J. Marians, Recruitment to stalled replication forks of the PriA DNA helicase and replisome-loading activities is essential for survival, DNA Repair (Amst.) 9 (2010) 202–209.
[8] R.C. Heller, K.J. Marians, Replication fork reactivation downstream of a blocked nascent leading strand, Nature 439 (2006) 557–562.
[9] M. Lopper, R. Boonsombat, S.J. Sandler, J.L. Keck, A hand-off mechanism for primosome assembly in replication restart, Mol. Cell 26 (2007) 781–793.
[10] C.J. Cadman, M. Lopper, P.B. Moon, J.L. Keck, P. McGlynn, PriB stimulates PriA helicase via an interaction with single-stranded DNA, J. Biol. Chem. 280 (2005) 39693–39700.
[11] J. Liu, P. Nurse, K.J. Marians, The ordered assembly of the phiX174-type primosome. III. PriB facilitates complex formation between PriA and DnaT, J. Biol. Chem. 271 (1996) 15656–15661.
[12] Y.H. Lo, K.L. Tsai, Y.J. Sun, W.T. Chen, C.Y. Huang, C.D. Hsiao, The crystal structure of a replicative hexameric helicase DnaC and its complex with single-stranded DNA, Nucleic Acids Res. 37 (2009) 804–814.
[13] S. Bailey, W.K. Eliason, T.A. Steitz, Structure of hexameric DnaB helicase and its complex with a domain of DnaG primase, Science 318 (2007) 459–463.
[14] K. Tougu, H. Peng, K.J. Marians, Identification of a domain of *Escherichia coli* primase required for functional interaction with the DnaB helicase at the replication fork, J. Biol. Chem. 269 (1994) 4675–4682.
[15] J. Dong, N.P. George, K.L. Duckett, M.A. DeBeer, M.E. Lopper, The crystal structure of *Neisseria gonorrhoeae* PriB reveals mechanistic differences among bacterial DNA replication restart pathways, Nucleic Acids Res. 38 (2010) 499–509.
[16] S. Shioi, T. Ose, K. Maenaka, M. Shiroishi, Y. Abe, D. Kohda, T. Katayama, T. Ueda, Crystal structure of a biologically functional form of PriB from *Escherichia coli* reveals a potential single-stranded DNA-binding site, Biochem. Biophys. Res. Commun. 326 (2005) 766–776.
[17] M. Lopper, J.M. Holton, J.L. Keck, Crystal structure of PriB, a component of the *Escherichia coli* replication restart primosome, Structure 12 (2004) 1967–1975.
[18] J.H. Liu, T.W. Chang, C.Y. Huang, S.U. Chen, H.N. Wu, M.C. Chang, C.D. Hsiao, Crystal structure of PriB, a primosomal DNA replication protein of *Escherichia coli*, J. Biol. Chem. 279 (2004) 50465–50471.
[19] D.L. Theobald, R.M. Mitton-Fry, D.S. Wuttke, Nucleic acid recognition by OB-fold proteins, Annu. Rev. Biophys. Biomol. Struct. 32 (2003) 115–133.
[20] A.G. Murzin, OB(oligonucleotide/oligosaccharide binding)-fold: common structural and functional solution for non-homologous sequences, EMBO J. 12 (1993) 861–867.
[21] C.Y. Huang, C.H. Hsu, Y.J. Sun, H.N. Wu, C.D. Hsiao, Complexed crystal structure of replication restart primosome protein PriB reveals a novel single-stranded DNA-binding mode, Nucleic Acids Res. 34 (2006) 3878–3886.
[22] M.R. Szymanski, M.J. Jezewska, W. Bujalowski, Interactions of the *Escherichia coli* primosomal PriB protein with the single-stranded DNA. Stoichiometries, intrinsic affinities, cooperativities, and base specificities, J. Mol. Biol. 398 (2010) 8–25.
[23] K.W. Chan, Y.J. Lee, C.H. Wang, H. Huang, Y.J. Sun, Single-stranded DNA-binding protein complex from *Helicobacter pylori* suggests an ssDNA-binding surface, J. Mol. Biol. 388 (2009) 508–519.
[24] S. Raghunathan, A.G. Kozlov, T.M. Lohman, G. Waksman, Structure of the DNA binding domain of *E. coli* SSB bound to ssDNA, Nat. Struct. Biol. 7 (2000) 648–652.

[25] C.C. Wang, H.W. Tsau, W.T. Chen, C.Y. Huang, Identification and characterization of a putative dihydroorotase, KPN01074, from *Klebsiella pneumoniae*, Protein J. 29 (2010) 445–452.
[26] C.Y. Huang, Y.W. Chang, W.T. Chen, Crystal structure of the N-terminal domain of *Geobacillus kaustophilus* HTA426 DnaD protein, Biochem. Biophys. Res. Commun. 375 (2008) 220–224.
[27] I. Wong, T.M. Lohman, A double-filter method for nitrocellulose-filter binding: application to protein–nucleic acid interactions, Proc. Natl. Acad. Sci. USA 90 (1993) 5428–5432.
[28] M. Abbani, M. Iwahara, R.T. Clubb, The structure of the excisionase (Xis) protein from conjugative transposon Tn916 provides insights into the regulation of heterobivalent tyrosine recombinases, J. Mol. Biol. 347 (2005) 11–25.
[29] T.L. Madden, R.L. Tatusov, J. Zhang, Applications of network BLAST server, Methods Enzymol. 266 (1996) 131–141.
[30] T.M. Lohman, M.E. Ferrari, *Escherichia coli* single-stranded DNA-binding protein: multiple DNA-binding modes and cooperativities, Annu. Rev. Biochem. 63 (1994) 527–570.